Experimental Proof for Electrochemical Non-Equilibrium Saturation Currents in Organic Crystals

F. Willig, G. Scherer, and W. Rothämel

Fritz-Haber-Institut der Max-Planck-Gesellschaft Berlin-Dahlem (Germany)

(Z. Naturforsch. **29 a**, 131–140 [1974]; received October 17, 1973)

For the same redox ion, diffusion controlled currents have been compared which were obtained at organic crystals and at a gold electrode. These experiments yield quantitative proof for electrochemical saturation currents in organic crystals with electrolytic contacts. Essential for this result is a modified voltage step method which enables an application of a high voltage simultaneous with the first contact between the crystal surface and the charge injecting electrolyte. The conditions necessary for the occurrence of a saturation current are discussed which also determine the electrochemical nature of this current corresponding to an ideal non-equilibrium between redox system and organic crystal.

Introduction

Since the first experiments by Kallmann and Pope in this field, it has been known that electrons can be transferred from organic crystals onto redox ions in solution [1]. Current-voltage curves measured at organic crystals with suitable electrolytic contacts exhibit two different regions corresponding to a space charge limited current at lower voltages and a current which is controlled by the supply of charge carriers at sufficiently high voltages [1, 2].

Negletcing an influence on the latter region from reactions of the injected charge carriers, Mehl has proposed that an electrochemical saturation current can be measured corresponding to the collection of all charge carriers formed per unit time through the electron transfer reaction at the crystal surface [3]. In their extensive study of injection currents in organic crystals with electrolytic contacts, Lohmann and Mehl found for defect electrons at the crystal surface a competition between a contribution to the injection current and a side reaction with solvent molecules leading to a deterioration of the crystal surface [4]. The latter was considerably reduced when a large voltage was applied to the crystal. Moreover, using a conventional voltage step method the authors discovered a diffusion controlled electron transfer from anthracene to $Ce(IV)/1.5\,N\,H_2SO_4$. The corresponding injection current was of a comparable magnitude as had been obtained for a diffusion controlled current of the same redox ion at a platinum electrode [4, 5]. Although we question the validity of the authors' assumption of a degenerate charge density at the crystal surface during this current measurement, we consider their experimental results to be the only strong support which has been given until now for the proposed occurrence of a saturation current in an organic crystal with electrolytic contacts. A quantitative decision on this point has not been reached in these experiments, however, since an oxidation of the electrodes could not be prevented in the case of anthracene or platinum. Correspondingly, an apparent diffusion coefficient derived for $Ce(IV)/1.5\,N\,H_2SO_4$ from a measurement with a rotating platinum electrode [5] is by 50 per cent smaller than that obtained at a gold electrode. In addition, in the experiment with the organic crystal the authors used a larger contact area for the injection of holes than for their discharge. Such a geometry of the electrodes is most convenient for electrolytic contacts but it will be shown in this paper that it leads to an apparent increase of a saturation current with rising voltage due to an increase in the effective area of the charge injecting contact.

The main purpose of this paper is to present quantitative experimental evidence for the occurrence of electrochemical saturation currents in organic crystals with electrolytic contacts. It will be shown that the application of a modified voltage step method is essential for the result since a conventional measurement of a current voltage curve can yield an artifact which differs by upto a factor of 10^3 from the actual saturation current. Necessary conditions for the occurrence of a saturation current will be discussed which also determine the electrochemical nature of this current corresponding to an

Sonderdruckanforderungen sind zu richten an Dr. F. Willig, Fritz-Haber-Institut der MPG, *D-1000 Berlin 33 (Dahlem)*, Faradayweg 4–6.

ideal non-equilibrium situation i.e. the absence of an equilibrium voltage drop in the Helmholtz-layer. A field dependent increase of electron transfer controlled saturation currents will be shown to arise from a voltage drop in the Helmholtz-layer due to the applied voltage.

Experimental

Materials

Thin organic crystals ($3-50\ \mu$) were grown from solution using chromatographically purified and zone refined materials. For each measurement a freshly grown crystal was used. The plate-like shape and the thinness of solution grown crystals is most suitable for an investigation of charge injection at the crystal surface since a large surface area (a, b-plane) and large field strengths are required. The average triplet lifetime of the anthracene crystals was 1 ms, that of the perylene crystals was only 8 μs. The lesser spectroscopic purity of solution grown crystals as compared to melt grown crystals is not expected to significantly affect the electron exchange at the crystal surface in the dark. All electrolytic solutions were prepared from p. a. substances and distilled water.

Apparatus

In Fig. 1 we have given an illustration of the modified voltage step method used in our experiments. A droplet of charge injecting solution is released from a pipette and first touches a platinum electrode connected to the high voltage supply before reaching the crystal surface (a, b-plane). Since the opposite crystal surface is already connected to the circuit, the high voltage is applied through the first contact between the charge injecting solution and the surface of a freshly grown crystal. The magnitude of the applied voltage is so chosen as to correspond to the saturation range of the current-voltage curve. To be able to vary the high voltage sufficiently fast during the measurement the voltage supply consists of a suitable pulse generator and a high voltage operational amplifier. The current is measured with a sensitive oscilloscope. Suitable contact materials for a discharge of the injected defect electrons at the opposite crystal surface do not exert any influence on the magnitude of the injection current, e.g. solutions of 10^{-2} N Fe(II)/1 M HCl or 10^{-2} M KCl serve the purpose. The time resolution of the method is limited by the time necessary for the spreading of the droplet on the crystal surface, typically less than 5 ms.

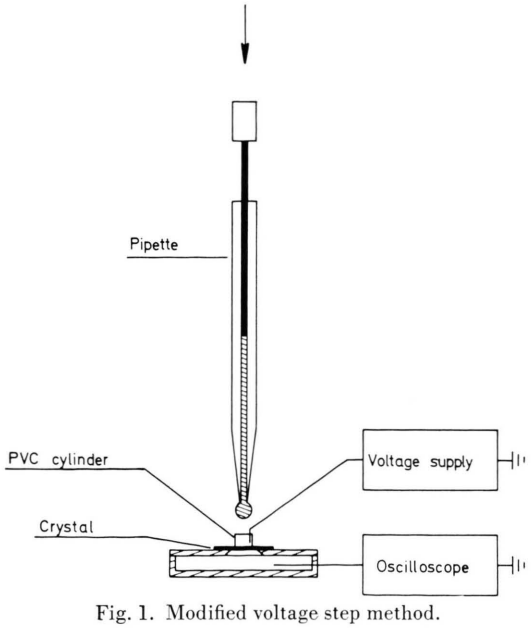

Fig. 1. Modified voltage step method.

Experiments

Diffusion Controlled Currents in an Organic Crystal and at a Metal Electrode

With a suitable combination of an organic crystal and a redox system in solution one can obtain a diffusion controlled generation of charge carriers at the crystal surface[6]. A measurement of a corresponding current is shown in the upper part of Fig. 2 for an injection of holes in an α-perylene crystal through 10^{-2} N Ce(IV)/2 N H_2SO_4. At constand applied voltage (shown in the lower part of Fig. 2) the current is inversely proportional to $\sqrt{t}$ as is expected for a diffusion controlled supply of charge carriers at a plain electrode[7]. A rise in the voltage results in a slight increase of the current. In this measurement the α-perylene crystal had a thickness of only 3.6 μ. A solution of 10^{-2} M KCl was used for the discharge of injected defect electrons at a circular contact area of 2 mm diameter which was half the diameter of the hole injecting contact. As will be shown below this particular geometry of the electrodes is responsible for the increase of the current with rising voltage observed in Figure 2.

In Fig. 3 a similar experiment is shown as in Fig. 2 but for an α-perylene crystal of 45 μ thickness. A much larger voltage had to be applied to this thicker crystal in order to obtain the same macroscopic field strength U/d_c (U = applied voltage, d_c = crystal thickness) as in the experiment

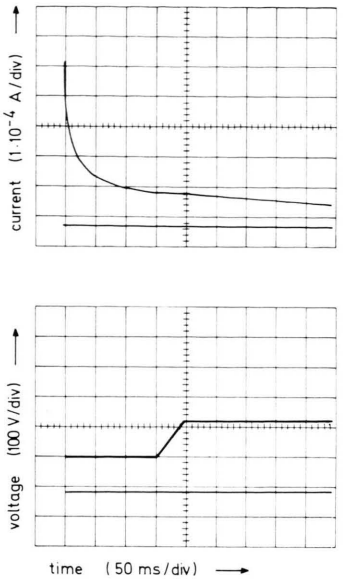

Fig. 2. Voltage dependence of the effective contact area for a diffusion controlled hole generation at a thin α-perylene crystal (3.6 μ), 10^{-2} N Ce(IV)/2 N H_2SO_4.

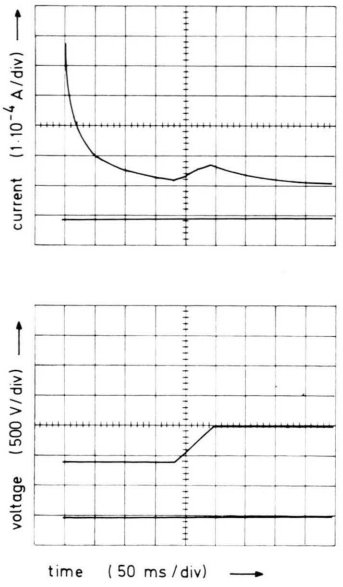

Fig. 3. Voltage dependence of the effective contact area for a diffusion controlled hole generation at a thick α-perylene crystal (45 μ), 10^{-2} N Ce(IV)/2 N H_2SO_4.

with the thinner α-perylene crystal. For the same macroscopic field strength the current is obviously larger for the thicker crystal than for the thinner one. However, in a number of such experiments with crystals of increasing thickness we have found the same dependence of the current on the applied voltage. The reason for this observation is simply a voltage dependent increase of the effective area of the charge injecting contact. Due to the steep voltage dependence in the space charge limited region of the current-voltage curve a significant contribution to the current flow only occurs from the area of the charge injecting contact which has already reached the saturation range. A rise in the voltage brings about an additional contribution to the saturation current also from geometric areas which lie further from the contact responsible for the discharge of the injected charge carriers at the opposite crystal surface. In almost all experiments with electrolytic electrodes such an unfavourable arrangement of the electrodes has been used until now. As a first approximation the voltage dependence of the saturation currents shown in Figs. 2 and 3 can be described by formula (A4) from the appendix.

$$I(U) = j_s \pi R^2 (1 + U(d_c/U_R R))^2 \qquad (A4)$$

for

$$U > U_R ;$$

I = current, U = applied voltage, j_s = current density of the saturation current, R = radius of the circular contact area responsible for the discharge of the charge carriers, U_R = minimum voltage necessary to reach the saturation range of the characteristic for an area of πR^2 of the injecting contact, d_c = crystal thickness.

Using formula (A4) a value of $U_R/d_c \approx 1 \times 10^5$ V/cm is obtained from a number of experiments as those shown in Figs. 2 and 3. A similar value for U_R/d_c has been found in experiments excluding the geometric effect (see below). In general the value of U_R/d_c depends on the magnitude of the saturation current and the occupancy of traps in the crystal bulk [compare inequality (1)].

As expected, this geometric effect does not occur when a smaller area is chosen for the injection of charge carriers than for their discharge. A corresponding experiment is shown in Fig. 4 for a diffusion controlled saturation current in an anthracene crystal of 18 μ thickness due to an injection of holes from 10^{-2} N Ce(IV)/conc. H_2SO_4. In this experiment a circular area for the hole injecting solution was limited to a diameter of 2 mm whereas the contact for the discharge of holes had a diameter of 6 mm. As shown in Fig. 4 with a such a geometry of the electrodes, the diffusion controlled current is independent of the applied voltage. In order to ob-

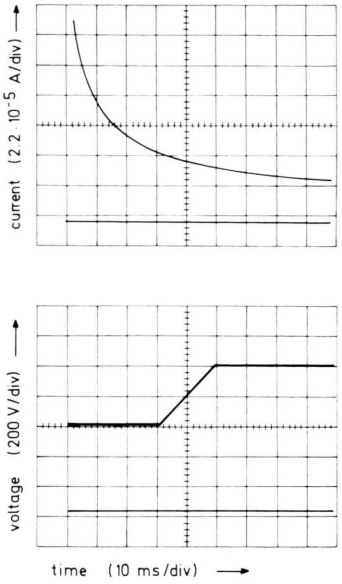

Fig. 4. Diffusion controlled hole saturation current in anthracene (20 μ), 10^{-2} N Ce(IV)/conc. H_2SO_4.

tain with Ce(IV) a diffusion controlled current in anthracene, a solution of concentrated H_2SO_4 has been used since a solution of Ce(IV)/2 N H_2SO_4 only leads to an electron transfer controlled current within this measuring time [6].

The observation of a diffusion controlled time dependence for an injection current in an organic crystal does not by itself prove the occurrence of an actual saturation current. Some fraction of the charge carriers generated at the crystal surface could still be consumed in a side reaction. Actual diffusion controlled saturation currents are known to occur at suitable metal electrodes [7]. In Fig. 5 such a diffusion controlled current is shown for 10^{-2} N Ce(IV)/2 N H_2SO_4 measured at a gold electrode at 0 V (SCE). We have obtained the same diffusion coefficient for ceric ions in H_2SO_4 from a voltage step measurement as shown in Fig. 5 and from a measurement with a rotating gold electrode [8]. The values of the diffusion coefficients measured at a gold electrode are larger by about 50 per cent than values derived from measurements at a rotating platinum electrode which is partially oxidized under such conditions [5]. For example, we have obtained at a gold electrode $D = 5.6 \times 10^{-6}$ cm^2/s for Ce(IV)/1 N H_2SO_4 and $D = 1.6 \times 10^{-6}$ cm^2/s for Ce(IV)/15 N H_2SO_4 as compared to values of 3.4×10^{-6} cm^2/s and 1×10^{-6} cm^2/s measured at a platinum electrode [5].

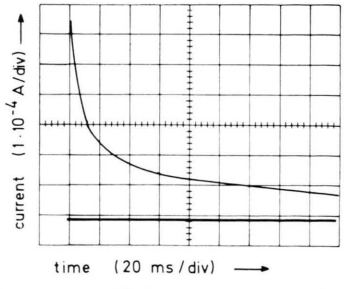

Fig. 5. Diffusion controlled current at a gold electrode 0 V (SCE), 10^{-2} N Ce(IV)/2 N H_2SO_4.

A comparison of the measurements shown in Fig. 2 for the thin α-perylene crystal and in Fig. 5 for the gold electrode reveals that indeed an actual saturation current has been measured in the organic crystal. A double logarithmic plot of both currents versus time is given in Figure 6. One can construct apparent current-voltage curves corresponding to the geometric effect, from the measurements shown in Figs. 2 and 3 by extrapolating to a common time base. To be able to apply formula (A4) from the appendix, the time base has to be chosen long as compared to the time at which the voltage had been raised to its final value. A further extrapolation to the voltage U_R of the equation (A4) then removes the geometric effect and yields the same current density for a diffusion controlled saturation current in an organic crystal and at a gold electrode which has the same dimensions as the contact used for the discharge of holes in the experiment with the organic crystal. As is obvious from Fig. 6 and formula (A4) such an extrapolation yields only a small correction for a very thin crystal but is rather significant for a thick crystal. For example, without

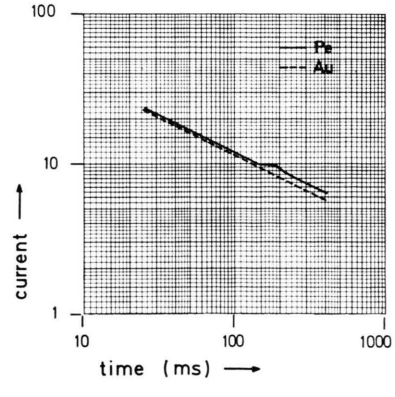

Fig. 6. Double logarithmic plot of current versus time for the measurements shown in Figs. 2 and 5.

such a correction a diffusion coefficient would be derived from the measurement shown in Fig. 3 which is 4 times larger than the correct value of $D = (5.0 \pm 0.3) \times 10^{-6}\,\mathrm{cm^2/s}$ obtained for Ce(IV)/2 N H_2SO_4 at a gold electrode. Such a geometric effect must have occurred in a number of experiments described in the literature, e.g. those reported by Lohmann and Mehl [4].

Field Dependence of Electron Transfer Controlled Saturation Currents

In Fig. 4 we have not observed any dependence of the current density on the applied voltage as is expected for a diffusion controlled saturation current. In contrast, with the same geometry of the electrodes as used in Fig. 4, the current density increases with rising field strength for an electron transfer controlled saturation current (Figure 7). This effect is independent of the crystal thickness and reflects a rise in the rate constant for electron transfer due to an increasing voltage drop in the Helmholtz-layer. It should not be confused with the voltage dependent geometric effect which is omitted in this experiment. The saturation current in Fig. 7 corresponds to an electron transfer from anthracene to 10^{-2} N Ce(IV)/2 N H_2SO_4. Since the crystal thickness was 18 μ, the macroscopic field strength was raised from 2.3×10^5 V/cm to 3.9×10^5 V/cm.

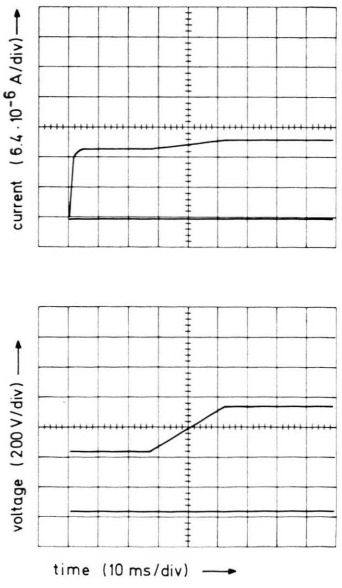

Fig. 7. Field dependence of an electron transfer controlled hole saturation current in anthracene (18 μ), 10^{-2} N Ce(IV)/2 N H_2SO_4.

The first steep rise of the saturation current reflects the spreading of the hole injecting solution on the crystal surface. In Fig. 7 one can observe that the corresponding charging current does not play any role in the measurement. The charging current is simply that occurring in a plate capacitor with growing area at constant field strength and can be calculated accordingly. It attains a maximum value of 7×10^{-7} A (about 1 mm in Fig. 7) at $t = 0$ and vanishes at $t = 4$ ms. For control purposes the charging current has been measured separately with a sufficiently small concentration of charge injecting species in the electrolyte.

Finally, we want to demonstrate the necessity for using the modified voltage step method in experiments with electrolytic contacts. In Fig. 8 we have plotted the results of two measurements which have been performed with freshly grown anthracene crystals and the same hole injecting solution of 10^{-2} N

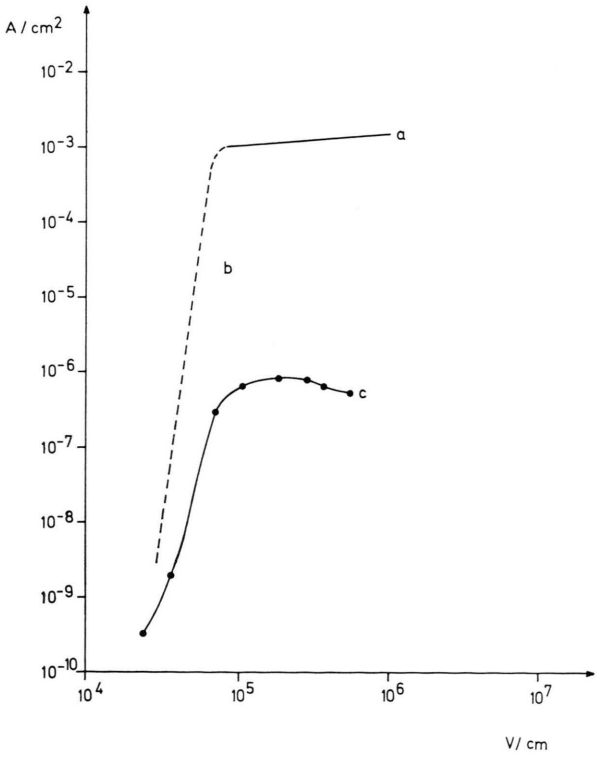

Fig. 8. Current density in anthracene versus macroscopic field strength U/d_c, U = applied voltage, d_c = crystal thickness, 10^{-2} N Ce(IV)/3.7 N H_2SO_4,
Curve a = modified voltage step method,
curve b = expected space charge limited current,
curve c = conventional measurement starting with zero voltage. Each point corresponds to a waiting time of 20 s.

Ce(IV)/3.7 N H_2SO_4. In Fig. 8 curve a has been obtained through a similar measurement as shown in Fig. 7, whereas curve c corresponds to a conventional experiment starting with zero applied voltage. In curve c each value of the current has been recorded 20 seconds after the voltage had been raised to its new value. A comparison of curves a and c shows that a severe deterioration of the crystal surface must have occurred during measurement c yielding an "apparent saturation current" which is too small by a factor of 10^3. The magnitude of this "apparent saturation current" is the same as has been reported for corresponding measurements in the literature [1, 3]. It should be noticed that the "apparent space charge limited current" in curve c is also an artifact since the deterioration of the crystal surface is progressing during the measurement. The actual space charge limited current is expected to be similar to the intermittant curve b. Thus, from a conventional current-voltage curve such as curve c one can neither determine the actual saturation current nor reliable parameters which should characterize a trap distribution for holes in the crystal bulk.

Discussion

We want to discuss the necessary conditions for the occurrence of a saturation current which also determine the electrochemical nature of this current. Due to the large band gap we only have to consider an electron exchange with the valence band of the organic crystal. In the absence of an external voltage an injection of holes leads to the formation of a positive space charge in the organic crystal and a negative counter charge in the electrolyte. To observe a net current flow an external voltage has to be applied to the crystal. When the following inequality (1) is valid, the sign of the field strength at the crystal surface is determined by this external voltage and is reversed as compared to a thermodynamic equilibrium situation.

$$\frac{U}{d_c} > \int \frac{\varrho}{\varepsilon_0 \varepsilon_c} \mathrm{d}x , \tag{1}$$

U = applied voltage, d_c = crystal thickness, ϱ = charge density, $\varepsilon_c, \varepsilon_0$ = dielectric constants of crystal and vacuum.

The integral is taken over the crystal thickness along the current path. Obviously, when inequality (1) is valid, the current is determined by the supply of charge carriers at the electrode.

Even in the case of a diffusion controlled current, within suitable time intervals we can assume a stationary distribution of charge carriers in the crystal. Therefore, we can write for the concentration of holes at the crystal surface:

$$\frac{\varrho_s}{e_0} = N \Big/ \left(1 + \frac{K_r(F) C_r(t) + K_s(F) C_s(t) + K(F, \varrho)}{K_0(F) C_0(t)} \right) \tag{2}$$

ϱ_s = charge density at the crystal surface, e_0 = elementary charge, $F = U/d_c$ = macroscopic field strength, t = time, N = density of states in the very narrow valence band, K_0 K_r, K_s = rate constants for ageneration, a back reaction and a side reaction of defect electrons at the crystal surface, C_0, C_r, C_s = concentration of oxidized and of reduced species of a redox system and of quenching molecules at the crystal surface. K = rate constant characterizing the transport of defect electrons from the crystal surface into the crystal bulk. In Eq. (2) traps can be considered by using a modified density of states.

When inequality (1) and Eq. (2) are valid, the injection current density j can be written as a product of two factors, a current density j_{ET} for the generation of holes at the phase boundary and a probability Y for a generated hole to contribute to the current flow.

$$j = j_{ET}\, Y = e_0 C_0(t) K_0(F) \cdot \left[N - \frac{\varrho_s}{e_0} \right] \left[1 \Big/ \left(1 + \frac{K_r(F) C_r(t) + K_s(F) C_s(t)}{K(F, \varrho)} \right) \right]. \tag{3}$$

We have seen in the experimental part that one can realize the following condition:

$$K_0(F)\,[N - \varrho_s/e_0] \gg \sqrt{D_0/t}\,. \tag{4}$$

D_0 = diffusion coefficient of the charge injecting species. In such a case we can substitute for j_{ET} in Eq. (3) [6]

$$j_{ET} = e_0 C_0^0 \sqrt{D_0/\pi t} \tag{5}$$

C_0^0 = concentration of the hole injecting species before the measurement. Under such an experimental condition we have been able to study the absolute magnitude and field dependence of the probability factor Y in Eq. (3) directly through a current measurement in an organic crystal without having to correct for the field dependence and magnitude of the hole generating reaction at the crystal surface. Making use of the fact that one can measure the

magnitude of the diffusion controlled current (5) at a metal electrode [7] we have found $Y = 1$ in Eq. (3) for diffusion controlled currents in α-perylene and anthracene crystals. Thus, the following inequality (6) is valid for saturation currents corresponding to $Y = 1$.

$$K(F, \varrho) \gg K_r(F) C_r(t) + K_s(F) C_s(t) \,. \qquad (6)$$

Obviously, using a modified voltage step method, an effect of a side reaction can be completely prevented. This is also true for a back reaction even when K_r is larger than in the experiments shown in this paper. Due to the strong dependence of the rate constants K_0 and K_r on the standard free energy of the reaction [6], a larger K_r is linked to a smaller K_0. Thus, in the case of a larger K_r, one can complete a measurement before any significant concentration of reduced species C_r has been produced and keep the effective rate constant $K_r C_r$ sufficiently small. Corresponding measurements will be discussed in detail elsewhere. Obviously, inequality (6) does not apply in the absence of an external voltage and also in the space charge limited range of the current-voltage curve. In this case a side reaction can lead to a serious deterioration of the crystal surface as has been shown in Figure 8. Therefore, to obtain an actual saturation current corresponding to the rate constant of electron transfer, one has to start a measurement in the saturation range of the current-voltage curve; i. e. one has to apply the modified voltage step method.

Inserting Eq. (2) into Eq. (3) we see that the validity of the following inequality (7) allows ϱ_s/e_0 to be neglected in comparison with N.

$$K(F, \varrho) \gg K_0(F) C_0(t) \qquad (7)$$

In this case we can derive the rate constant $K_0(F)N$ for the generation of holes directly from the magnitude of an electron transfer controlled saturation current without having to correct for ϱ_s. Since under our experimental conditions we can neglect a back reaction and a side reaction; the charge density should increase when a greater number of holes is generated per unit time at the crystal surface. Thus, if inequality (7) would not be valid according to Eq. (3) we should find a relative decrease in the magnitude of the saturation current for the increasing charge density ϱ_s. However, in all cases we have found a linear increase of the saturation current when the concentration of oxidized species C_0 was enhanced over a wide range, e. g. 10^{-6} N to 10^{-1} N Ce(IV)/3.7 N H_2SO_4.

Using inequalities (6) and (7) the electron transfer controlled saturation current shown in Fig. 7 can be described by the following formula (8):

$$j = j_{ET} = e_0 C_0^0 N K_0^0 (1 + \gamma (U/d_c)) \qquad (8)$$

with $K_0^0 = K_0(\eta = 0)$, η = voltage drop in the Helmholtz-layer.

In the absence of a specific adsorption of ions at the surface of the organic crystal, we can determine the rate constant $K_0^0 N$ corresponding to electron transfer in the absence of a voltage drop in the Helmholtz-layer simply by extrapolating to zero applied voltage, obtaining in this case $K_0^0 N = 4.3 \times 10^{-4}$ cm/s. The ideal non-equilibrium situation between the organic crystal and the redox system in solution stemming from the validity of inequalities (1), (6) and (7) leads to a strong dependence of the rate constant $K_0^0 N$ on the standard free energy of the reaction [6]. It shall be mentioned that in contrast an exchange current at a metal electrode is determined for an equilibrium voltage drop in the Helmholtz-layer and thus is independent of the standard free energy of the reaction. The linear increase of the saturation current in Fig. 7 reflects an increase of the rate constant for electron transfer due to a rising voltage drop η in the Helmholtz-layer. If we assume the same exponential relationship as observed for a larger change in η at a metal electrode [7], we can consider Eq. (8) as a corresponding linear expansion.

$$\gamma \frac{U}{d_c} = \frac{\alpha e_0 \eta}{k_B T} = \frac{\alpha e_0 \delta_H \varepsilon_c}{k_B T \varepsilon_H} \left(\frac{U}{d_c} - F_h \right), \qquad (9)$$

α = transfer coefficient, k_B = Boltzmann constant, T = temperature, $\eta = (\varepsilon_c/\varepsilon_H)\delta_H (U/d_c - F_h)$ voltage drop in the Helmholtz-layer, $U/d_c - F_h$ = effective field strength at the crystal surface, ε_c, ε_H = dielectric constants of crystal and Helmholtz-layer, δ_H = thickness of the Helmholtz-layer.

Inserting in Eq. (9) $\alpha = 1$, $U/d_c > F_h$, $\delta_H = 3$ Å, $\varepsilon_c = 3.4$ for anthracene and the experimental value $\gamma = 7 \times 10^{-7}$ cm/V, we obtain $\varepsilon_H \approx 6$ as an estimate for the dielectric constant in the Helmholtz-layer of the system. This value would indicate a partial orientation of water molecules at the surface of the organic crystal. Accordingly, we obtain $\eta \approx U \delta_H/d_c$ 1.7 = 7 mV for $\delta_H = 3$ Å and $U/d_c = 4 \times 10^5$ V/cm in the experiment shown in Figure 7.

In Eq. (3) we have used a phenomenological description of the probability Y of a charge carrier to escape from the crystal surface. The rate constant $K(F, \varrho)$ contains all the unspecified physical details. Until now one has not arrived at a detailed formulation of this probability Y. However, the main contributing factors can be discussed separately. If one can neglect an attractive force acting on the charge carrier due to its localized counter charge and its image charge, and in addition neglect the space charge; a charge carrier would only experience an attraction due to the macroscopic field strength U/d_c. A corresponding implicit assumption $K(F) = \mu(U/d_c)$ has been made by Mehl and Hale in their treatment of injection currents [9]. Taking e. g. $\mu = 0.5\ \mathrm{cm^2/Vs}$ and $U/d_c = 5 \times 10^5\ \mathrm{V/cm}$, such an assumption yields $K = 2.5 \times 10^5\ \mathrm{cm/s}$ which is larger than the collision frequency $Z = 10^4\ \mathrm{cm/s}$ for a redox ion at a plain electrode [10]. Thus, one would expect $Y = 1$ even for the maximum possible rate constant for the back reaction.

On the other hand, a simple point charge model yields the following attractive field strength F_A as experienced by a positive point charge at the center of a surface molecule when its negative counter charge is located at the outer Helmholtz-plane.

$$F_A = \frac{e_0}{8\pi\varepsilon_0 h^2(\varepsilon_c + \varepsilon_E)} + \frac{e_0(\varepsilon_E - \varepsilon_c)}{16\pi\varepsilon_0 h^2(\varepsilon_c + \varepsilon_E)} - \left(\frac{U}{d_c} - F_h\right) \qquad (10)$$

ε_E = effective dielectric constant of the electrolyte and h = distance of both point charges from the phase boundary. For simplicity we have assumed the same distance $h = 3$ Å from the Helmholtz-plane to the phase boundary and from there to the centre of a surface molecule (a, b-plane of an anthracene crystal). The first term in equation (10) stems from the counter charge, the second term from the image charge, and in the third term the field U/d_c stemming from the external voltage is reduced by a field F_h due to the positive space charge in the crystal. The attractive field strength F_A of Eq. (10) corresponds to the bottom of a potential well for the charge carrier. However, when the positive point charge is shifted into the crystal bulk, Eq. (10) has to be modified and the corresponding potential cannot be derived simply from an integration of Equation (10). Nevertheless, it is sufficient to consider the general form of the terms in Eq. (10) in order to state the main factors determining the depth of the potential well. If we insert in Eq. (10) $h = 3$ Å, $\varepsilon_c = 3.4$ for anthracene, and the static dielectric constant of water $\varepsilon_E = \varepsilon_s = 78$, we obtain from each of the first two terms a contribution $f_A \geqq 10^6\ \mathrm{V/cm}$ which has to be compared with the smallest macroscopic field strength $U/d_c = 1 \times 10^4\ \mathrm{V/cm}$ for which we have already measured saturation currents, i. e. $Y = 1$ in Eq. (3), with the modified voltage step method at low injection levels.

For the image charge term such a static point charge model has been considered by Kallmann and Pope in their first discussion of injection currents [11]. In a recent discussion of conventionally measured current-voltage curves Michel-Beyerle and Haberkorn have pointed that a fast Brownian motion of the charge carrier as compared to a slow relaxation time for water dipoles leads to a decrease in the effective dielectric constant for the image charge term [12]. For holes in anthracene mobilities of $0.5\ \mathrm{cm^2/Vs}$ in c'-direction and $2\ \mathrm{cm^2/Vs}$ in b-direction [13], along with lattice parameters of 11 Å and 6 Å, yield jumping probabilities of about 10^{13}/s and 10^{14}/s which are large compared to a reciprocal dielectric relaxation time of 10^{+11}/s for water dipoles. Thus, water dipoles only experience an electric field from a positive charge which is spread over more than 100 crystal molecules. It appears difficult at present to obtain a good estimate of the residual image charge which can follow the individual jumps of the charge carrier. Taking the infrared dielectric constant of water $\varepsilon_E = \varepsilon_{IR} = 4.5$ and $\varepsilon_c = 3.4$ for anthracene, the attractive field at the crystal surface due to the image charge should be $3 \times 10^5\ \mathrm{V/cm}$ and it should vanish completely if the optic dielectric constant $\varepsilon_E = \varepsilon_0 = 1.8$ should apply.

Even for $\varepsilon_E = \varepsilon_s = 78$, the first term in Eq. (10) yields an attractive field strength $f_A = 10^6\ \mathrm{V/cm}$ and the counter charge cannot be assumed to be screened simply by water molecules as has been suggested by the same authors [12]. This value even has to be considered as a lower limit since a much smaller value $\varepsilon_H = 6$ is indicated for the dielectric constant of the Helmholtz-layer by the field dependence of the electron transfer controlled saturation current in Figure 7. For $F_A \geqq 10^6\ \mathrm{V/cm}$ and the minimum value $U/d_c = 1 \times 10^4\ \mathrm{V/cm}$ for which we have observed a saturation current the attraction experienced by the charge carrier from its localized counter charge is balanced by the external field at a distance larger than 50 Å

from the counter charge. Therefore, there is a large probability for the injected charge carrier to return to the bottom of the potential well at the crystal surface (Figure 8). It is at first surprising to observe under such conditions $Y = 1$ in Equation (3). However, in the present experiments we have used charge injecting solutions of large ionic strength corresponding to a small Debye screening length. Thus, a screening of the localized counter charge can take place when by virtue of its Brownian motion the charge carrier has moved some distance away from it. Once the localized counter charge has been screened by the ionic cloud, the charge carrier experiences only a much weaker attraction from a counter charge which is now spread over a fairly large surface area. This is the case again, since the relaxation time of an ionic cloud is large (e. g. $\Theta = 8 \times 10^{-12}/c \approx 10^{-11}$ s with $c = 2$ moles/liter H_2SO_4 [14]) compared to the average time the charge carrier is bound to an individual crystal molecule; i. e. 10^{-14} to 10^{-13} s. Therefore, for the described modified voltage step experiments with a charge injecting contact of large ionic strength we shall neglect the existence of a localized counter charge since we know from our experiments that the charge carrier does not undergo any reaction during the screening time of this localized counter charge. If in addition we assume a sufficiently small image charge as a first approximation we only have to consider a homogenous field strength at the crystal surface and can thus write in Eq. (3):

$$K(F, \varrho) = \mu (U/d_c - F_h) \qquad (11)$$

μ = mobility of the charge carrier.

The field strength F_h includes contributions from the positive space charge in the crystal and from the delocalized counter charge and image charge. Evidently, the value of F_h increases with the magnitude of the saturation current and the occupancy of traps in the crystal. Considering the minimum value of $U/d_c = 1 \times 10^4$ V/cm for which we have observed a saturation current in our anthracene crystals and $\mu = 0.5$ cm^2/Vs for holes in c'-direction we find under our experimental conditions $K_r C_r$, $K_s C_s$, $K_0 C_0 \ll 5 \times 10^3$ cm/s.

At small ionic strengths a charge carrier is expected to be bound to its localized counter charge for a much longer time than at large ionic strength and the chance for an involvement in a back reaction or side reaction should be enhanced. However, if both these reactions are sufficiently slow, a saturation current can occur also in this case since the charge carrier can eventually escape due to its Brownian motion and that of the ion carrying the counter charge. Until now, cases with $Y < 1$ have not been studied under well defined experimental conditions with electrolytic contacts. However, cases with a small probability for an injected charge carrier to contribute to the current flow have been reported for other contact materials. Recently, a steep linear increase of a photocurrent with rising voltage has been reported to arise for a field dependent escape of a charge carrier from a localized counter charge in a dielectric medium (fatty acid layer) at the phase boundary [15]. The authors applied the same model for ionic recombination which has been shown to describe photocurrents generated in the crystal bulk [16]. However, the solution of the model, a Bessel function of zeroth order [17], would predict a non-linear increase (by more than 60 per cent at 10^5 V/cm) over the linear field dependence which has been observed in the experiment. Therefore, the interpretation of this experiment should be modified. In general however, well defined experiments with a probability $Y < 1$ for charge separation should reveal some details about the interaction of the injected charge carrier with the phase boundary.

Acknowledgement

We wish to thank Prof. H. Gerischer for his support and valuable advice.

Appendix

Voltage Dependent Effective Surface Area

The geometric effect shown in Figs. 2 and 3 is due to the steep voltage and thickness dependence of a space charge limited current [2] in contrast to a saturation current (compare Figure 8).

$$j_{SCL} \sim \frac{U_S^{l+1}}{S^{l+1}} \qquad (A\,1)$$

j_{SCL} = space charge limited current density, U_S = voltage drop along the current path, S = length of the current path, l = parameter characterizing the trap distribution for the charge carriers in the crystal, e. g. $l = 5$.

We define U_R as the minimum voltage necessary to reach the saturation range with current density j_S

when both the contact areas, for injection and discharge of the charge carriers, are of the same magnitude πR^2. When the same voltage U_R is applied to the same system but with a larger radius $R_i > R$ for the charge injecting contact, the current can be described by the formula:

$$I(U_R) = j_s \pi R^2 + \int_R^{R_i} j_{SCL}(r)\, 2\pi r \, dr \qquad (A\,2)$$

with $R_i > R$.

The radius r originates in the centre of the charge injecting contact. In the second term most contributions from the space charge limited current flow correspond to a much longer current path S than that of the saturation current in the first term $S \approx r - R \gg d_c$, where d_c is the crystal thickness. Therefore, considering formula (A 1) and Fig. 8 as a first approximation we can neglect the second term in Eq. (A 2) completely in comparison to the first term. When the voltage in the system is now raised to a value $U_2 > U_R$, the saturation range is also obtained for all current paths with length $S \leqq S_2 = R_2 - R$ where R_2 is defined by the following expression:

$$U_R/d_c = U_2/(R_2 - R). \qquad (A\,3)$$

Similar arguments apply to the current $I(U_2)$ as have been given for $I(U_R)$. From the ratio of both currents we obtain the voltage dependence of the current in the system (at constant current density j_S).

$$I(U_2) = I(U_R)\left(1 + U_2(d_c/U_R R)\right)^2 \qquad (A\,4)$$

for

$$U_2 > U_R .$$

Obviously, one can make a number of refinements in the above derivation. We want to mention the following three additions to our simple argument. When the electron transfer reaction is diffusion controlled the width of the diffusion layer for the injecting redox ion in solution is narrower close to a section of the charge injecting contact, which corresponds to a space charge limited current flow, than close to a section which corresponds to a saturation current. Therefore, immediately after the voltage has been raised in such a system a larger increase in the magnitude of the current is expected to occur than is predicted by formula (A4). Long after the change in the voltage, formula (A4) is applicable again. On the other hand for an electron transfer-controlled saturation current one has to consider in Eq. (A4) the actual field dependence of the rate constant itself leading to a voltage dependent current density j_S (Figure 7). Finally, in conventional measurements (curve c in Fig. 8) the geometric effect is often obscured due to a drastic deterioration of the crystal surface during the experiment.

[1] M. Pope, H. P. Kallmann, A. Chen, and P. Gordon, J. Chem. Phys. **36**, 2486 [1962].
[2] P. Mark and W. Helfrich, J. Appl. Phys. **33**, 205 [1962].
[3] W. Mehl, Ber. Bunsenges. physik. Chem. **69**, 583 [1965].
[4] F. Lohmann and W. Mehl, Electrochimica Acta **13**, 1469 [1968].
[5] R. Greef and H. Aulich, J. Electroanal. Chem. **18**, 295 [1968].
[6] F. Willig, G. Scherer, and W. Rothämel, Ber. Bunsenges. physik. Chem., to be published.
[7] H. Gerischer and W. Vielstich, Z. physik. Chem., N. F. **3**, 16 [1955].
[8] W. Rothämel, Thesis TU München 1973.
[9] W. Mehl and J. M. Hale, in Advances in Electrochemistry and Electrochemical Engineering, ed. P. Delahay and C. W. Tobias, Vol. 6, p. 399, Interscience, New York 1967.
[10] R. A. Marcus, J. Chem. Phys. **43**, 679 [1965].
[11] H. P. Kallmann and M. Pope, J. Chem. Phys. **36**, 2482 [1962].
[12] M. E. Michel-Beyerle and R. Haberkorn, Z. Naturforsch. **27 a**, 1496 [1972].
[13] J. Fourny and G. Delacote, J. Chem. Phys. **50**, 1028 [1969].
[14] H. Falkenhagen, Theorie der Elektrolyte, p. 119, S. Hirzel, Stuttgart 1971.
[15] H. Killesreiter and H. Bässler, Phys. Stat. Sol. (b) **53**, 193 [1972].
[16] R. H. Batt, C. L. Braun, and J. F. Hornig, J. Chem. Phys. **49**, 1967 [1968].
[17] L. Onsager, Phys. Rev. **54**, 554 [1938].